Chapter 1

The Standard Model and Physics of the Top Quark

1.1 The Standard Model

The Standard Model is the name given to the theory developed during the course of the 20th century, which describes the elementary particles that make up all known, observable matter, and the three fundamental forces they interact by (electromagnetic, weak and strong forces). The Standard Model does not, however, describe the gravitational force as it is difficult to model mathematically at a quantum scale. The Standard Model puts forward twelve fermions, with a spin quantum number of $\frac{1}{2}$, as the matter particles, split into two groups of six quarks and six leptons, all of which are split into three generations. The six quarks are classified according to their charge and flavour: up, down, charm, strange, top and beauty quarks. The leptons are in turn classified according to their charge and flavour: electron, muon or tau leptons, together with their corresponding neutrinos). Neutrinos, although originally thought to be massless, are now believed to carry mass due to the observation of the oscillation of neutrinos between different flavours. Table 1.1 shows these particles of the Standard Model in their respective generations in tabular form. All of these particles

have a respective antiparticle which has identical quantum numbers except opposite electric charge.

Generation	Flavour	Charge / e	Spin	Mass /MeV
		Leptons		
I	electron (e)	-1	$\frac{1}{2}$	0.511
	electron neutrino (ν_e)	0	$\frac{1}{2}$	0
II	muon (μ)	-1	$\frac{1}{2}$	105.66
	muon neutrino (ν_μ)	0	$\frac{1}{2}$	0
III	tau (τ)	-1	$\frac{1}{2}$	105.66
	tau neutrino (ν_τ)	0	$\frac{1}{2}$	0
		Quarks		
I	up (u)	$+\frac{2}{3}$	$\frac{1}{2}$	$2.3^{+0.7}_{-0.5}$
	down (d)	$-\frac{1}{3}$	$\frac{1}{2}$	$4.8^{0.5}_{-0.3}$
II	charm (c)	$+\frac{2}{3}$	$\frac{1}{2}$	$(1.275^{+0.025}_{-0.025}) \times 10^3$
	strange (s)	$-\frac{1}{3}$	$\frac{1}{2}$	95^{+5}_{-5}
III	top/truth (t)	$+\frac{2}{3}$	$\frac{1}{2}$	$(173.21 \pm 0.51 \pm 0.71) \times 10^3$
	bottom/beauty (b)	$-\frac{1}{3}$	$\frac{1}{2}$	$(4.18^{+0.03}_{-0.03}) \times 10^3$
		Bosons		
Force	Gauge Boson(s)	Charge / e	Spin	Mass / GeV
Weak	$W^+/W^-/Z^0$	+/-/0	1	$80.385 \pm 0.015/91.188 \pm 0.002$
Electromagnetic	photon (γ)	0	1	0
Strong	gluon (g)	0	1	0
Gravitation	graviton	0	1	0
-	Higgs (H)	0	0	125.7 ± 0.4

Table 1.1: Fundamental fermions, split into their three generations, and bosons of the Standard Model. Particle properties taken from [22].

All known, observable matter in the universe is composed of the aforementioned twelve fermions or their antiparticles. The only particles which are stable are the proton, which is made of two up quarks and a down quark; the neutron, which is made of one up quark and two down quarks; and the electron. All other particles are unstable and decay; they are produced only in particle colliders such as the Large Hadron Collider, or in cosmic radiation. Quarks also carry the charge of the strong force, termed 'colour', of red, green or blue. The only quark which does not 'hadronise' (form bound colourless states) is the top quark which has a very short lifetime of $\approx 5 \times 10^{-25} s$ [22] due to its large mass.

These fermions interact via the integer spin (spin 1) gauge bosons of the three fundamental forces. Electron, muon and tau leptons interact via the electromagnetic and weak forces; their neutrinos, since they carry no electric charge, interact only via the weak force; and the quarks interact via the electromagnetic, weak and strong forces. Each of the forces are mediated by gauge bosons that are the 'force carriers', and lead to the formation of hadrons and atoms. The mediator of the strong force is known as the gluon, that of the electromagnetic force is the photon and those of the weak force are the W^+, W^- and Z bosons. Table 1.1 shows the gauge bosons and their properties.

The range of action of the boson determines the interaction range of the force it carries. Heavier bosons, like the W^+, W^- and Z bosons, have a short range of action, while massless bosons such as photons and gluons have a theoretically infinite range. In reality, this is not the case because the gluons themselves carry the strong colour charge and so interact with each other, reducing their interaction range. The range of the fundamental forces is quantified by their coupling strength, denoted α. Taking the strength of the strong force as the baseline, the relative strength of the electromagnetic force is 10^{-2}, that of the weak force is 10^{-13} and the strength of the gravitational force is 10^{-42} [16]. The electromagnetic coupling strength, also known as the fine-structure constant, is defined at low energies as $\alpha_{em} = \frac{e^2}{4\pi} \approx \frac{1}{137}$. Although the strong force is the strongest force, it has a limited range of only an estimated 10^{-15}m, and the weak force has an estimated range of 10^{-18}m, while the electromagnetic and gravitational forces have infinite range.

The Higgs boson, whose discovery was announced in July 2012 by the CMS and ATLAS experiments at the LHC, is the latest component of the Standard Model to be discovered [9, 1]. The mechanism of electroweak symmetry breaking through which other particles acquire mass is due to this Higgs field.

1.1.1 Gauge Principle

The underlying mathematical model of the Standard Model is a Quantum Field Theory (QFT) combining special relativity and quantum mechanics. All interactions in the the SM must conserve the kinematic quantities energy and momentum. In addition, the electromagnetic and strong forces conserve the dynamical quantities charge, colour, baryon number, lepton number and quark flavour. The weak force, if mediated by a charged propagator ($W^{\pm}$), can allow the violation of quark flavour, meaning a quark can decay into another flavour quark.

The laws of conservation occur as a result of underlying symmetries in the theories; for instance, energy conservation stems from time symmetry and angular momentum conservation is a result of rotational symmetry. In addition to these classical symmetries, a quantum field theory can also possess gauge symmetries. The principle of gauge invariance refers to field theories in which the Lagrangian, which summarises the dynamics of the system, is invariant under local transformations (transformations that are a function of, and therefore different at all space-time points in, a field). The collection of all such transformations, called gauge transformations, are called the Lie group. If the Lie group is commutative, i.e. any order of application of the symmetry transformations produces the same result, the theory is termed Abelian. Conversely, if the group is non-commutative, the theory is non-Abelian. Each Lie group has an associated generator, and each generator has a corresponding vector field, or gauge field, whose purpose is ensuring invariance under local transformations. The quanta of these fields are the gauge bosons of the Standard Model. Note that the converse of local transformations are global transformations, in which the transformation takes place instantaneously at all space-time points.

Group transformations can be represented as groups of $n \times n$ matrices which possess properties such as unitarity (U) and orthogonality (O). A group of matricies with determinant 1 is called 'special' (S), leading to further groups of $SU(N)$ and $SO(N)$. The Standard Model is comprised of electroweak theory (combining electromagnetism and weak theory) a gauge

group of $SU(2) \times U(1)$ and the theory of strong interactions that has a gauge symmetry of $SU(3)$. The Standard Model is therefore a gauge theory based on the gauge group $SU(3) \times SU(2) \times U(1)$.

1.1.2 Quantum Electrodynamics

Quantum electrodynamics (QED) is a component theory of the Standard Model that governs the interactions of electrically charged particles. The simplest electromagnetic process is shown in Figure 1.1a, and all real processes are made of some number of these processes combined together, such as electron-positron annihilation shown in Figure 1.1b.

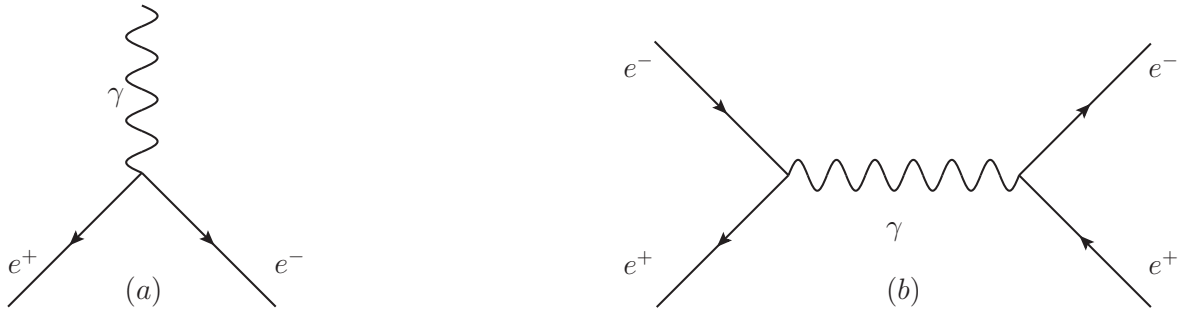

Figure 1.1: (a) the elementary electromagnetic process of an electron emitting a photon and (b) electron-positron annihilation.

The sum of all possible orders of Feynmann diagrams for a possible interaction is the representation of the real process. In practice, since at low energies, each vertex contributes a factor of α ($= \frac{1}{137}$, the fine structure constant, the coupling constant of the electromagnetic force), additional Feynmann diagrams with more than a few vertices contribute negligibly to the process and are often ignored.

The coupling strength of a force can be further explained in terms of vacuum polarisation. This refers to the phenomenon of electron-positron pairs and photons being spontaneously created and absorbed by an electron. These virtual particles, which would be represented in Feynmann diagrams as closed loops, shield the original electron leading to the electron charge being measured at a lower value than its true charge. This measured value is called

the effective, or 'screened', charge. As a result, the coupling strength of the electromagnetic force decreases as a function of distance.

The mathematical formulation of QED stems from the Dirac equation, which describes the Lagrangian for a spin-half (Fermionic) field ψ.

$$\mathcal{L} = i(\hbar c)\bar{\psi}\gamma^{mu}\partial_{\mu}\psi - (mc^2)\bar{\psi}\psi \tag{1.1}$$

Here, $\hbar$ is the reduced Planck's constant, μ are the Lorentz indices and γ^{mu} are the gamma (or Dirac) matrices. Under a global transformation of a phase $i\alpha$,

$$\psi(x) \to \psi'(x) = e^{i\alpha}\psi(x), \bar{\psi} \to \bar{\psi}'(x) = e^{-i\alpha}\bar{\psi}(x) \tag{1.2}$$

this Lagrangian is invariant (i.e. under a global transformation of the $U(1)$ group, since this is equivalent to multiplication of the field ψ by a 1×1 unitary matrix). However, under a local gauge transformation by a phase of $i\alpha(x)$, the symmetry is no longer true since the partial derivative

$$\partial_{\mu}(e^{i\alpha(x)}\psi) = i(\partial_{\mu}\alpha(x))e^{i\alpha(x)}\psi + e^{i\alpha(x))}\partial_{\mu}\psi, \tag{1.3}$$

meaning the Lagrangian is not invariant:

$$\mathcal{L} \to \mathcal{L} - \bar{\psi}(x)\gamma^{\mu}\psi(x)[\partial_{\mu}\alpha(x)]. \tag{1.4}$$

Local symmetry can be maintained in this case if a new gauge field, A_{μ}, is introduced to the

Lagrangian by means of a covariant derivative D_μ:

$$D_\mu = \partial_\mu + ieA_\mu. \tag{1.5}$$

Under the local transformation, A_{mu} tranforms as

$$A_\mu \to A'_\mu = A_\mu - \frac{1}{e}\partial_\mu \alpha(x). \tag{1.6}$$

If the partial derivatives in the Dirac equation are now replaced with the covariant derivatives, the invariant Lagrangian is obtained:

$$\mathcal{L} = i(\hbar c)\bar{\psi}\gamma^{mu}\partial_\mu\psi - e\bar{\psi}\gamma^\mu\psi A_\mu - (mc^2)\bar{\psi}\psi - \frac{1}{4}F^{\mu\nu}F_{\mu\nu}. \tag{1.7}$$

In this way, the principle of local gauge invariance under the $U(1)$ group is used to obtain the final Lagrangian, that of quantum electrodynamics. The physical interpretation of the gauge field A_μ is the photon, which couples to charged particles (electrons and positrons) with a coupling strength proportional to the charge. The term $\frac{1}{4}F_{\mu\nu}$ is an additional term to account for the kinetic energy of the free particle of the new gauge field, i.e. the photon; and there is no term giving the photon mass.

In this way, the principle of local gauge invariance under the $U(1)$ group is used to introduce additional fields to a Lagrangian in order to make it covariant with respect to a group $U(1)$ local gauge invariance

1.1.3 Electroweak Theory

The unification of the electromagnetic and weak forces in the 1960s provided a more complete theory of fundamental particles. This unification takes the form of an $SU(2) \times U(1)$ gauge

group correlating the electromagnetic and weak forces, and can be constructed in a similar way to the QED formalism in Section 1.1.4.

First, it is necessary to define isospin, I an abstract fundamental property of fundamental particles that is conserved in weak interactions. Similarly, weak hypercharge, Y is also a quantum property, defined as $Y_W = 2(Q - I_3)$, where Q represents the charge of the particle and I_3 is the third component of isospin. I_3 takes a value of $\frac{1}{2}$ for up, charm and top quarks and for neutrinos; and $-\frac{1}{2}$ for down, strange, beauty and other leptons other than neutrinos.

It has been shown empirically that the weak interaction exhibits violation of parity (P) and interacts only with left-handed particles via the charged gauge bosons ($W^{\pm}$). Hence, the fields representing fermions are split into left handed and right handed components by defining a left handed doublet containing the left handed electron and left handed neutrino, and a right handed singlet containing the right handed electron:

$$\chi_L = \begin{pmatrix} \nu_e \\ \\ e \end{pmatrix}_L , e_R \tag{1.8}$$

Here, the left handed doublet has $I = \frac{1}{2}$, and the right handed lepton has $I = 0$. Similar doublets can be constructed for the other generations of leptons (μ and τ) and quarks in their pairs of three generations (ud, cs and tb). Right handed neutrinos, which would have $I = 0$ and $Y = 0$, do not exist in the Standard Model.

Four additional massless fields and their associated currents are introduced in order to impose invariance: W^1_μ, W^2_{mu}, W^3_{mu} and B_μ. The W_μ fields form a triplet that transforms according to the $SU(2)$ group, and undergoes interactions with the third isospin component I_3. The B_μ field similarly transforms by the unitary group $U(1)$, and interacts with the weak hypercharge Y. These additional fields lead to the construction of three weak isospin currents and a weak hypercharge current.

Requiring local gauge invariance under a the $SU(2) \times U(1)$ group, the covariant derivative is

$$D_\mu = \partial_\mu + \frac{i}{2} g_W \vec{\tau} \cdot \vec{W}_\mu + i g' \frac{Y}{2} B_\mu. \tag{1.9}$$

The vectors W^1_μ, W^2_μ, W^3_μ have coupling strengths of g_W to the three isospin currents and B_μ couples to the hypercharge current with a strength of g'. These four bosons relate to the quanta of the new fields, i.e. the gauge bosons $W^\pm$, Z^0 and γ. In actual fact, the $W^\pm$ bosons are linear superpositions of the W^1_μ and W^2_μ states, while the neutral states W^3_μ and B_μ undergo a mixing related by the weak mixing angle, θ_W, to give the neutral Z^0 and γ bosons. The coupling constants of the electromagnetic and weak forces are related by the weak mixing angle, by $tan\theta_W = \frac{g'}{g_W}$.

It has been experimentally observed that both W bosons and the Z boson have mass. Indeed, the strength of the electromagnetic force is of the same order as the weak force, but as a result of the weak gauge bosons having mass, the weak force appears weaker and has a shorter range. However, the local gauge invariance would be broken if terms are now included to give the bosons mass. The theory of spontaneous breaking of the symmetry underlying the $SU(2) \times U(1)$ group addresses this problem, as explained in Section 1.1.5.

The weak force has been shown to change the flavour of quarks in an interaction, meaning flavour conservation is broken []. As stated, the quarks, like leptons, come in the form of left handed doublets within each generation,

$$\begin{pmatrix} u_L \\ d'_L \end{pmatrix}, \begin{pmatrix} c_L \\ s'_L \end{pmatrix}, \begin{pmatrix} t_L \\ b'_L \end{pmatrix} \tag{1.10}$$

with isospin $\frac{1}{2}$. Note that the lower quarks of the doublets are denoted with primes as they indicate a rotated state of the quark, called Cabibbo-rotated states, which are superpositions of the physical quarks. This means that in, for example, the decay of a down quark to an up quark via emittance of a W^-, the down quark to which the W^- couples is actually a superposition of 'down type' quarks, i.e. down, charm and beauty quarks. The Cabbibo-

Kobayashi-Maskawa matrix (CKM), relates the weak interaction mixed states to the physical quark states. This is the degree of quark mixing between the different generations, and results in the measured values below of $|V_{12}|$ for the probability of a transition from quark 1 to quark 2 in a weak interaction [22]. In reference to top physics, the $|V_{tb}|$ value of almost 1 means that the top quark almost always decays to a W boson and a b-quark.

$$\begin{pmatrix} V_{\mathrm{ud}} & V_{\mathrm{us}} & V_{\mathrm{ub}} \\ V_{\mathrm{cd}} & V_{\mathrm{cs}} & V_{\mathrm{cs}} \\ V_{\mathrm{td}} & V_{\mathrm{ts}} & V_{\mathrm{tb}} \end{pmatrix} = \begin{pmatrix} 0.974 & 0.225 & 0.004 \\ 0.225 & 0.973 & 0.041 \\ 0.009 & 0.041 & 0.999 \end{pmatrix} \tag{1.11}$$

1.1.4 Quantum Chromodynamics

In the theory of quantum chromodynamics (QCD), the charge of the strong force is colour, and the force is independent of other particle properties such as charge and flavour. Empirical data has led to the conclusion that there are three colour charges: red, green and blue [16]. While the colour of a quark can be changed in a strong interaction, colour conservation is a requirement of strong processes (just as charge conservation in QED). The mediators of the strong force, gluons, carry a positive and a negative colour charge themselves, and so can interact directly with other gluons. The coupling constant of the strong force is a 'running' coupling constant, meaning that it varies depending on the distance between the particles undergoing the interaction. At small distances of the order of the size of the proton ($\tilde{0}$.1 fm), α_S is small and becomes larger as distance increases, leading to quarks and gluons being essentially free particles and interacting weakly with each other when confined within a hadron, a phenomenon termed asymptotic freedom.

The previously mentioned colourless bound quark states are called hadrons. The process in which free gluons and quarks form bound colourless states is called hadronisation and manifests as a cone of particles, termed jets. Hadrons are divided into two types: mesons are composed of a quark and an antiquark with the quark carrying a colour charge and

the antiquark carrying the respective anticolour; baryons are composed of three quarks or three antiquarks. Recently, the LHCb experiment at CERN published first results of the observation of a pentaquark state [3] TODO:WORTH MENTIONING?

The proton, a baryon, consists of two u-quarks, one d-quark and gluons binding the qquarks together. However, the structure of the proton becomes more complicated, consisting of more particles, as the momentum of the probing particle increases. The aforementioned three-quark-structure of the proton is evident at low momenta, while at higher momenta, virtual pairs of quarks, antiquarks and gluons are visible. These virtual quarks and gluons are termed sea-quarks and make up most of the mass of the proton. In any proton, its constituent particles each carry some fraction, x, of the overall proton momentum.

The quantum field theory of QCD is determined to have an underlying symmetry of the group $SU(3)$, based on the fact that there are three colour charges. Imposing local gauge invariance, the Lagrangian contains eight generators of the $SU(3)$ group. These generators lead to eight gauge fields, whose physical interpretation are the eight massless gluons that mediate the strong force. Therefore, although in principle there could be nine gluons, since there are three colours and gluons carry a positive aqnd a negative colour charge, the $SU(3)$ symmetry leads to a colour octet and a colour singlet. TODO: COULD STATE THEM HERE BUT DON'T THINK IT'S NECESSARY.

Any particle that occurs in nature must be a colour singlet, and so the gluons in the colour octet are never seen in nature. However, although the final gluon is a colour singlet, it has not been observed and is thought not to exist. If it did exist, it would result in a long range strong force, but it is known that the strong force has a short range of action.

1.1.5 Spontaneous Symmetry Breaking

The spontaneous breaking of the electroweak $SU(2)$ symmetry mentioned in Section 1.1.3, also known as the Higgs mechanism was put forward in the 1960s [17]. This theory was put

forward as a mechanism by which the $W^{\pm}$ and Z gauge bosons could acquire mass, since the Lagrangian of the electroweak interaction contains no mass term for these particles, and their inclusion would violate local gauge invariance.

The method by which this symmetry is spontaenously broken begins with the inclusion of two new complex scalar 'Higgs' fields (so in total there are four components to these two complex fields). The introduction of these fields results in an additional scalar potential energy term in the Lagrangian, $V(\Phi)$, where Φ represents the newly introduced complex scalar fields. The potential $V(\Phi)$ is defined as

$$V(\Phi) = -\mu^2\Phi^\dagger\Phi + \lambda^2(\Phi^\dagger\Phi)^2 \tag{1.12}$$

Imposing the requirement of μ^2 and λ both being greater than 0 (WHY?), gives a potential of the geometry shown in Figure 1.2. The minimum of this potential is clearly not at $\Phi = 0$, rather, the minimum has a circular form given by the formula $\Phi^\dagger\Phi = \frac{\mu^2}{2\lambda} = \frac{v^2}{2}$, where $v = \frac{|\mu|}{\sqrt{\lambda}}$, the 'vacuum expectation value' of the Higgs. Since the minimum, i.e. the vacuum, is at a location other than $\Phi = 0$, The new field is said to have a non-zero vacuum expectation value, and the $SU(2) \times U(1)$ symmetry is spontaneously broken. The observed Higgs boson is created as a result of perturbations in the potential about this minimum, which removes three of the four Φ components, with the remaining field being the scalar Higgs field. In addition to this new particle, introducing the new fields also results in the fields associated with the $W^{\pm}$ and Z^0 bosons in the Lagrangian acquiring mass.

Terms known as Yukawa coupling terms can be introduced to specify the interactions of Φ with the fermion fields. It is this coupling of the Higgs field to any massive particle that gives them a proportional mass. The top quark, being the heaviest known particle at 173 GeV, has a Yukawa coupling to the Higgs close to 1.

Results published at the discovery of the Higgs boson are shown in Figure 1.3 in the Higgs$\rightarrow \gamma\gamma$ and Higgs$\rightarrow$ ZZ channels. These plots of the invariant masses of the $\gamma\gamma$ and ZZ combinations show a clear excess of events around 125 GeV. The latest results from CMS and ATLAS

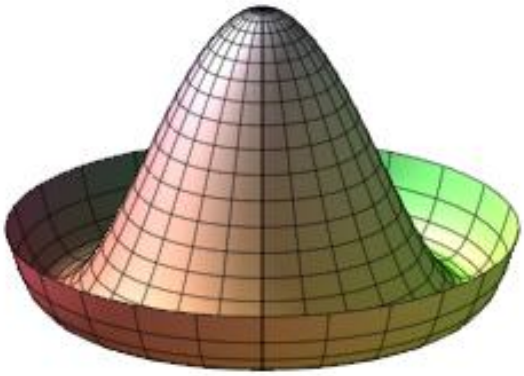

Figure 1.2: The Higgs field potential $V(\Phi)$ [20].

state a Higgs mass of $125.09 \pm 0.21 \pm 0.11$ GeV [2], where the first uncertainty is statistical and the second is systematic. Since the announcement of the discovery of the Higgs boson in 2012, studies have continued to determine its quantum properties. Thus far, results show it to be in agreement with predictions from the Standard Model.

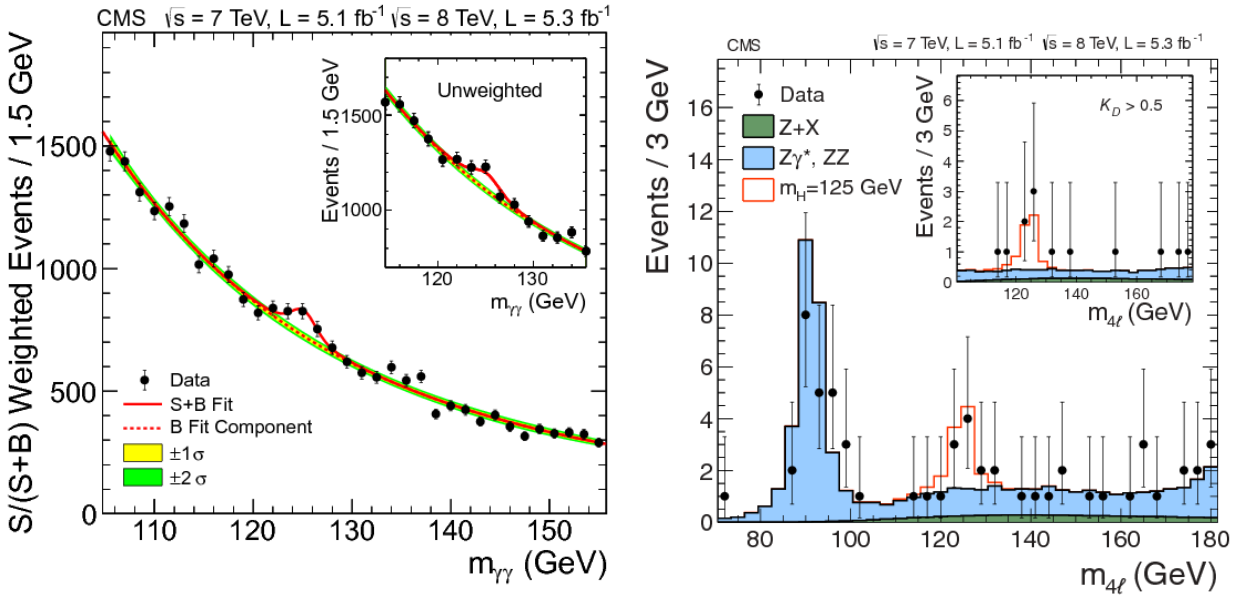

Figure 1.3: Invariant mass in $H \to \gamma\gamma$ (left) and $H \to \mathrm{ZZ}$ (right) channels [9].

1.2 Incompleteness of, and physics beyond, the SM

The Standard Model has proven to be an extremely successful theory thus far. However, its inability to describe many phenomena in the universe lead to it being considered currently incomplete. Indeed, a 'Grand Unified Theory' combining the electromagnetic, weak and strong interactions is considered to be the ultimate aim, with all of these forces being different physical manifestations of one single force.

There are many free parameters in the Standard Model and the very reason why it takes the form it has, with four fundamental forces, six quarks and six leptons, each divided into three generations, is not explained. The gravitational force is also conspicuous by its absence from the SM. The imbalance between matter and anti-matter in the universe, despite the generally accepted view that both were created in equal quantities in the Big Bang, is also not explained by the SM. Although the evident matter-antimatter asymmetry in the unvierse could be partially explained by the observed charge-parity (CP) symmetry violation in weak interactions [10], this is not sufficient to account for the observed excess.

Neither does the SM provide a theoretical explanation for neutrino mass. Originally thought to be massless, neutrinos are now thought to have mass, albeit extremely small, based on observations of neutrino oscillations between different flavours [19, 15].

The hierarchy problem, in terms of the Higgs boson, is the name given to the fact that the Higgs mass is so much smaller than the predicted value of the order of the Planck scale ($1.22 \times 10^{19}\,\text{GeV}$). The observed mass is the sum of the bare particle mass and any corrections from high order processes. This disagreement suggests that there occurs some 'fine tuning' of the bare Higgs mass to lead to the measured mass of approximately 125 GeV.

Supersymmetry (SUSY) is one potential solution to hierarchy problem. This theory proposes a symmetry between fermions (spin $\frac{1}{2}$) and bosons (spin 1). Each particle has an associated 'superpartner' with identical quantum properties with the exception of spin, which differs by $\frac{1}{2}$, so that all Standard Model fermions have a boson superpartner, and all Standard Model

bosons have a fermion superpartner. These super particles, or sparticles, are thought to have higher masses than their Standard Model counterparts since they have not been discovered yet. If this is the case, supersymmetry would be a broken symmetry. In many supersymmetry theories, the lightest SUSY particle (LSP) is stable and is a potential candidate to be a dark matter particle.

Dark matter and dark energy are thought to constitute about 27% dark matter, 68% dark energy and 5% ordinary matter (Figure 1.4) [6]. The origins and nature of the dark energy and dark matter are currently unknown and they are as yet unobserved, but their existence has been inferred from their gravitational effects on galactic masses composed of stars, gases and dust. The relatively large amounts of dark matter and dark energy hypothesised suggests that they are made up of weakly interacting massive particles.

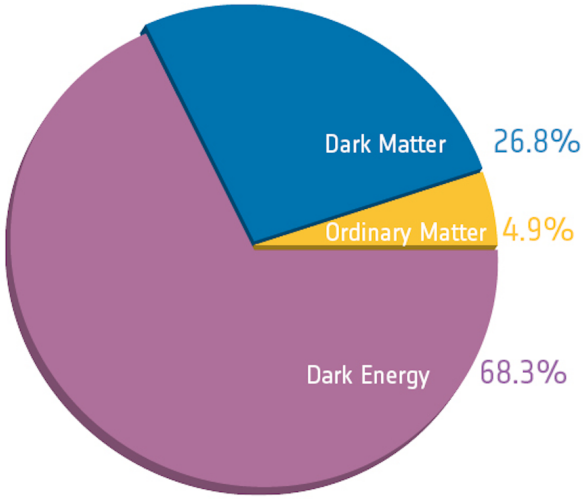

Figure 1.4: The composition of the universe showing the amounts of dark matter, dark energy and ordinary matter based on latest results from Planck/ESA [6]

1.3 Top Physics at the LHC

The top quark was discovered by the CDF and DØ collaborations in 1995 [5, 4] and is still one of the less well studied fundamental particles in the Standard Model. The top quark is the heaviest fermion with its mass currently placed at $173.29 \pm 0.23(stat.) \pm 0.92(syst.)$ GeV/c^2

[11]. Since the lifetime of the top quark is very short, approximately 5×10^{25} s [22], it is the only one of the quarks to decay before it hadronises, meaning that the bare quark properties can be investigated. These unique properties of the top quark within the Standard Model mean it is an interesting focus of study.

1.3.1 Top Quark Production and Decay

Top quarks can be produced either in top-antitop ($t\bar{t}$) production through the strong interaction or single top (t-quark) production through the electroweak mechanism. During Run 1 of data taking at the LHC produced millions of top quark pair events with gluon-gluon fusion or quark-antiquark annihilation being the primary production mechanisms, as shown in Figure 1.5. Gluon-gluon fusion dominates at the LHC since protons are collided with protons, meaning antiquarks are only available from sea quarks in the proton. In addition, at low momentum fractions, x, the gluon density in the proton is large compared to the sea quarks, and increases at a higher rate than that of the sea quarks. TODO: COULD INSERT PLOT OF PROTON PDFs IF NEEDED

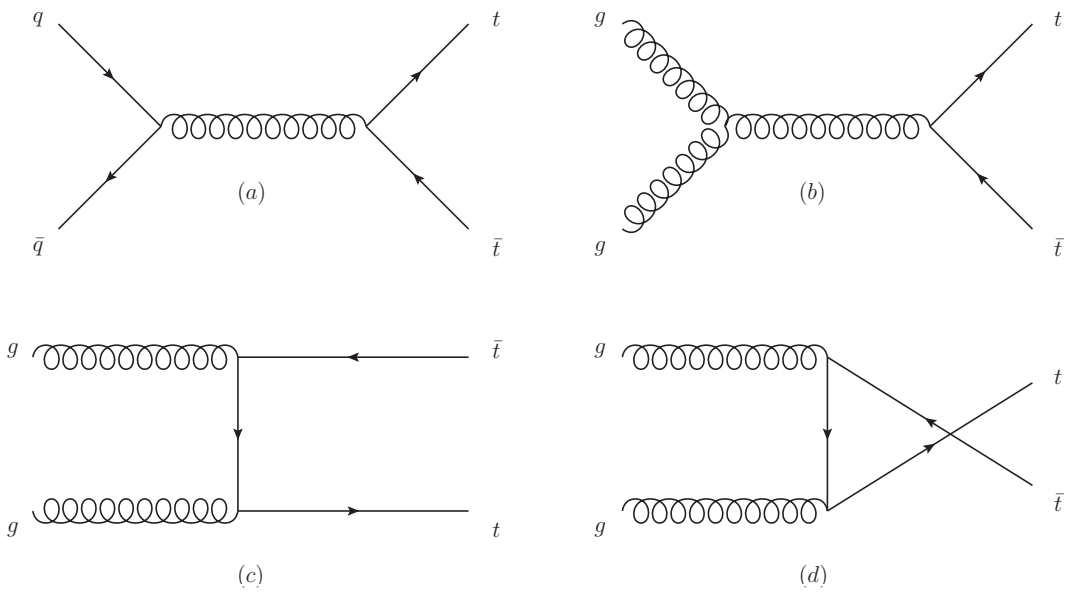

Figure 1.5: Feynman diagrams of leading order $t\bar{t}$ production processes. (a) depicts quark-antiquark annihilation, and (b, (c) and (d) depict gluon-gluon fusion in the s, t and u channels respectively.)

At $\sqrt{s} = 7\,\text{TeV}$, gluon-gluon fusion accounts for approximately 80% of the total t-quark production cross section, increasing to approximately 90% at $\sqrt{s} = 14\,\text{TeV}$ [22].

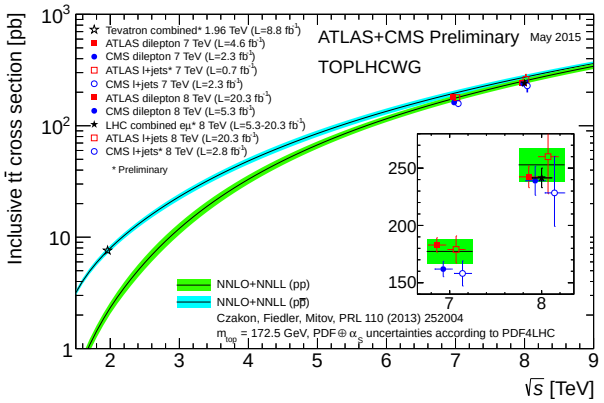

Figure 1.6: $\text{t}\bar{\text{t}}$ production cross sections at 1.96 TeV at CDF and DØ at the TeVatron and at 7 TeV and 8 TeV at CMS and ATLAS at the LHC. HOW REFERENCE IMAGE FROM https://twiki.cern.ch/twiki/bin/view/LHCPhysics/TopLHCWGSummaryPlots?

Top quarks decay almost 100% of the time to a W-boson and a b flavour jet. The W-boson then decays either hadronically (into two jets) or leptonically (lepton + neutrino). Top pair events are characterised by the decay of the W-bosons:

- Leptonic: $\text{t}\bar{\text{t}} \rightarrow \text{W}^+\text{bW}^-\bar{\text{b}} \rightarrow l\nu_l\text{b}l'\bar{\nu}_{l'}\bar{\text{b}}$. Both W-bosons decay to a lepton and a neutrino. The event would consist of 2 jets, 2 leptons and 2 neutrinos (which would show up as $E_{\text{T}}^{\text{miss}}$ in the event). (10.5%)

- Hadronic: $\text{t}\bar{\text{t}} \rightarrow \text{W}^+\text{bW}^-\bar{\text{b}} \rightarrow \text{q}\bar{\text{q}}\text{bq}\bar{\text{q}}\bar{\text{b}}$. Both W-bosons decay to two jets. The event would consist of 6 jets. (45.7%)

- Semi-Leptonic: $\text{t}\bar{\text{t}} \rightarrow \text{W}^+\text{bW}^-\bar{\text{b}} \rightarrow \text{q}\bar{\text{q}}\text{b}l\nu_l\bar{\text{b}}$. One W-boson decays to a lepton and a neutrino, the other decays to two jets. The event would consist of 4 jets, 1 lepton and 1 neutrino. This decay is shown in Figure 1.7. (43.8%)

The branching ratios for each decay mode are quoted in brackets [22], and are represented graphically in Figure 1.8. The numbers of jets in the final state of each channel could be higher than the numbers quoted above as a result of higher order processes such as initial state radiation (radiation from the gluons before the $\text{t}\bar{\text{t}}$ production) or final state radiation.

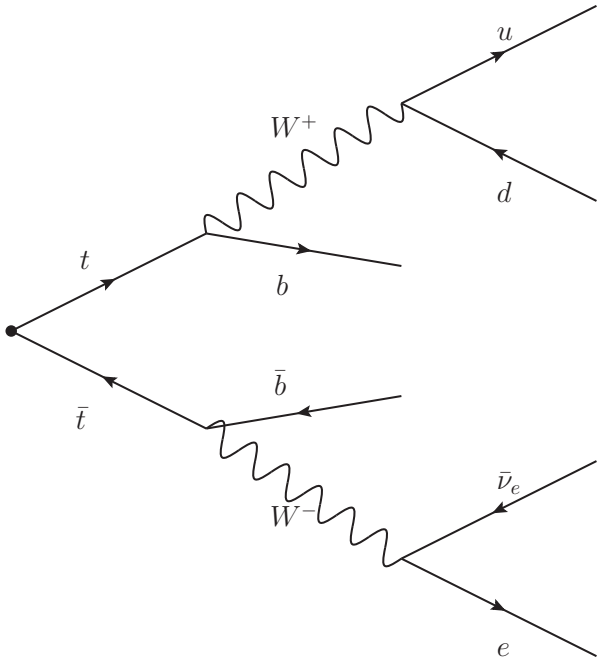

Figure 1.7: Feynman diagram of the electron+jets semi-leptonic $t\bar{t}$ decay channel

The hadronic decay channel, with multiple jets and no leptons in the final state, is difficult to distinguish from the QCD multijet, W+jets and Z+jets backgrounds. Conversely, the leptonic channel has a very clean signature with two leptons, however the low branching ratio would limit the available statistics. The semi-leptonic channel, with one lepton and four jets provides a good balance between statistics and event identification. The lepton can be any of an electron, muon or τ, but τs are not included in semi-leptonic t-quark analyses in general as they are difficult to identify (see Section **??**).

The signal event for this analysis is the semi-leptonic channel of the $t\bar{t}$ decay, also referred to as the lepton+jets channel, where the lepton is either an electron or a muon. These channels have a branching ratio of apprimxately 14.2 % and 14.4 % respectively [22].

1.3.2 Single Top background

Single top production is one of the backgrounds considered in this analysis, and can occur via the electroweak interaction in one of three channels: s-channel or t-channel which involve

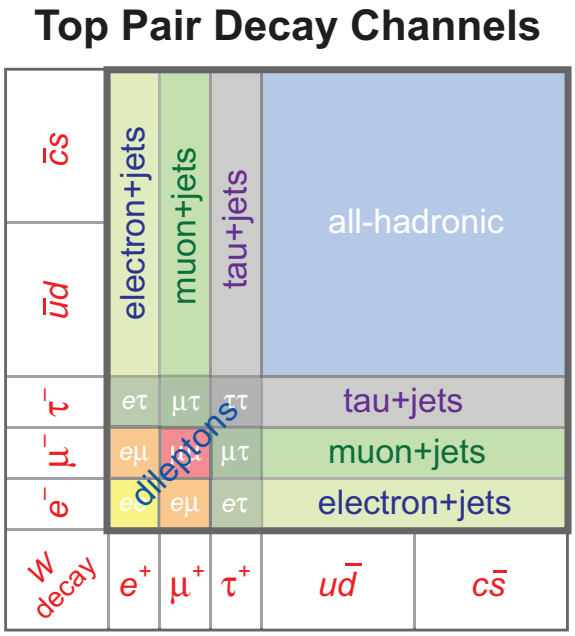

Figure 1.8: Relative branching ratios of the $t\bar{t}$ system

the exchange of a virtual W boson, or tW-channel which involves the associated production of a W boson and a top quark. Although semi-leptonic $t\bar{t}$ decays have more jets in the final state than these single top production modes, initial state radiation and final state radiation, where low energy gluons and quarks are produced before and after the interaction that produces the single quark, can increase the numbers of jets in single top events. This can lead to such events having a similar signature to $t\bar{t}$ events, and providing a non-negligble background.

1.3.3 W/Z+jets background

W+jets events present a significant background to semi-leptonic $t\bar{t}$ analyses. This background consists of events in which a real W boson is produced together with additional jets. Events in which these W bosons decay leptonically, can provide a similar event signature after reconstruction to that of a semi-leptonic $t\bar{t}$ decay. However, in general, these processes can be removed from the signal selection because the final decay products in W + jets events have lower energies than those from semi-leptonic $t\bar{t}$ decays, since the top quark has a high mass.

Another characteristic of W + jets events is that the jets are more likely to be light quark jets and therefore less likely to be the necessary b-jet s from $t\bar{t}$ events. Thus, W + jets events can be separated from the $t\bar{t}$ signal by using jet multiplicity, jet p_T and b-jet multiplicity.

Similarly, Z + jets events can mimic $t\bar{t}$ events where the leptonic decay of Z bosons to a lepton and an anti-lepton takes place. This background can be distinguished and removed from semi-leptonic $t\bar{t}$ decays by vetoing on a second lepton and imposing jet multiplicity requirements. Misidentification and misreconstruction of these leptons as jets, however, such events could appear to be $t\bar{t}$ events and pass the signal selection, although this contamination would be small.

1.3.4 QCD background

The multi-jet background from QCD events is also a significant background to this semi-leptonic $t\bar{t}$ analysis. Gluon-gluon fusion and quark-antiquark annihilation in proton-proton collisions can produce energetic jets. Although these processes have only two jets in their final state, higher order processes, including initial state radiation and final state radiation, can also produce additional jets, leading to potential mimicking of the semi-leptonic $t\bar{t}$ signal. The leptons required for this to happen can come from jets which are misreconstructed and misidentified as leptons, or real leptons in heavy flavour (b and c flavour) jets. Unfortunately the cross section of these processes is much higher (by several orders of magnitude) than the signal cross section. Although the lepton (either fake or real) is rarely one that passes selection, the much higher QCD cross section means that its contribution as a background is significant.

In the muon+jets channel, only highly energetic jets (p_T >500 GeV) are capable of ''punching through'' from the calorimeters to leave tracks in the muon chambers. Such events can be removed by isolation (since it deposits significant amounts of energy in the calorimeters) requirements. Events with real electrons and muons from heavy quark jets can be identified

by the track quality requirements in the selection since they would not begin from the primary vertex and so would have a distrinct track signature compared to prompt leptons.

On the other hand, the electron channel poses a more problematic QCD background, due mainly to the conversion of photons, whether produced at the interaction point or through subsequent decays and radiation, into electrons and positrons. The identification and removal of such events is described in Section **??**. However, the large uncertainty in the cross section of QCD events, large contamination from higher order processes with additional jets in the signal region of this analysis and the difficulty in Monte Carlo modelling of such contributions lead to significant disagreements in the numbers of events passing the signal selection in data and in simulation. Therefore, the QCD background is modelled using a data driven method.

The QCD background is difficult to model precisely because of large uncertainties on the cross sections and the significant higher contributions which can easily be mismodelled, leading to incorrect event kinematics and selection biases. Hence, the QCD background shape is modelled using a data driven method, decribed in Section **??** and then normalised to the number of events passing the selection process in Monte Carlo.

1.4 Monte Carlo Simulation

Monte Carlo event simulation is used to simulate the aforementioned signal and background processes, and to compare the theoretical knowledge of the Standard Model incorporated therein with real data. Differences between simulation and data would then indicate the presence of new physics processes which are not present in the theoretical assumptions made in the Standard Model, or perhaps that the simulation process is sub-optimal. Different event generators exist, and samples produced by the MadGraph, PYTHIA, POWHEG and HERWIG generators are used in this analysis.

Different generators have characteristics which optimise them for different aspects of the production chain: the initial hard process scattering of the partons in the hadrons (protons), decay showers of the resulting partons, subsequent decays of resulting hadrons and hadronisation of resulting partons, and the underlying event (the parton showers produced from soft scattering between the remaining contents of the colliding protons).

1.4.1 MadGraph

MadGraph [8], a matrix element generator, works by taking into account every potential Feynman diagram for a given process and subsequently calculating the matrix elements for said diagrams over all phase space. The parton distribution functions are used to generate the incoming partons. The cross section of the process and various subprocesses and the structure and contents of the event (such as the partons present and their kinematics) are thus produced. Proton fragmentation and subsequent hadronisation are simulated using the PYTHIA generator, as explained in Section 1.4.3. The parton showers are then matched with the matrix element partons via the MLM method [18]. This method ensures that parton showers with a highly energetic jet are not double counted.

Matching is then carried out between parton showers in the hadronisation and the partons from the matrix element calculations. The matching is carried out by satisfying distance requirements in η and ϕ between the parton and parton shower. Only if the parton has a transverse energy above a certain threshold, is it considered for this matching, and if an event contains either too few or too many matching jets, it is discarded. The matching threshold is process dependent as follows:

- $t\bar{t}$: 20 GeV
- W + jets: 10 GeV
- Z + jets: 10 GeV

1.4.2 MCatNLO

The MC@NLO [12, 14] generator is a next-to-leading-order generator. These aditional corrections provide more accurate simulations of physics processes in comparison to leading-order generators by including additional partons from the initial hard process in the final state of the event.

1.4.3 PYTHIA

PYTHIA [23] then simulates the proton fragmentation, the subsequent hadronisation of the resulting quarks and gluons resulting from the hard interaction and the underlying event. PYTHIA is considered to be particuarly good at multi-particle simulation, modelling fragmentation and hadronisation, and matching parton showers. Therefore, PYTHIA carries out these steps after the initial partons are provided by other generators in most simulated samples, if it is not already used for the whole production chain (as is common in QCD multijet simulations).

1.4.4 POWHEG

One problem with the MC@NLO generator is that some events are given negative weights when matching the next-to-leading-order QCD multijet calculations to parton showers. The Positive Weight Hardest Emission Generator, POWHEG [13, 21, 7], is another next-to-leading-order generator which generates the hardest processes in the event first, which avoids double counting of softer radiation produced later in the chain, which is the cause of negative event weights.

1.5 Theoretical Systematics

1.5.1 Factorisation & Matching Threshold

Systematic uncertainties are present in the choice of the threshold transverse energy above which matching of matrix element partons to parton showers is carried out. Simulated samples, in which the threshold is increased and decreased by a factor of 2, are used to estimate the affect of this uncertainty on this analysis:

- $t\bar{t}$
  - + variation: 40 GeV
  - - variation: 10 GeV
- W + jets
  - + variation: 20 GeV
  - - variation: 5 GeV
- Z + jets
  - + variation: 20 GeV
  - - variation: 5 GeV

Similarly, the factorisation scale at which α_S is varied up and down from the nominal value of $Q^2 = m^2 + \Sigma p_T^2$ by a factor of 2 to produce simulation samples to evaluate the sytematic uncertainty resulting from this. The uncertainty resulting from these variations are evaluated in both $t\bar{t}$ and W/Z + jets processes.

1.5.2 Detector Simulation (GEANT)

Following creation of the physics processes in proton-proton collisions, the simulated events are then put through a detector simulation to evaluate the interation of the detector with the products of collisions. The Geometry and Tracking 4 (GEANT4) package is used for this purpose, which generally simulates what happens to particles as they travel through the geometry of the detector, including simulation of the detector components and materials and the interaction of particles with the detector such as particle tracks and energy deposits.

References

[1] Georges Aad et al. Observation of a new particle in the search for the Standard Model Higgs boson with the ATLAS detector at the LHC. *Phys. Lett.*, B716:1--29, 2012.

[2] Georges Aad et al. Combined Measurement of the Higgs Boson Mass in pp Collisions at $\sqrt{s} = 7$ and 8 TeV with the ATLAS and CMS Experiments. *Phys. Rev. Lett.*, 114:191803, 2015.

[3] Roel Aaij et al. Observation of $J/\psi p$ resonances consistent with pentaquark states in $\Lambda_b^0 \to J/\psi K^- p$ decays. 2015.

[4] S. Abachi et al. Observation of the top quark. *Phys.Rev.Lett.*, 74:2632--2637, 1995.

[5] F. Abe et al. Observation of top quark production in $\bar{p}p$ collisions. *Phys.Rev.Lett.*, 74:2626--2631, 1995.

[6] P.A.R. Ade et al. Planck 2013 results. I. Overview of products and scientific results. *Astron.Astrophys.*, 571:A1, 2014.

[7] Simone Alioli, Paolo Nason, Carlo Oleari, and Emanuele Re. A general framework for implementing NLO calculations in shower Monte Carlo programs: the POWHEG BOX. *JHEP*, 1006:043, 2010.

[8] J. Alwall, R. Frederix, S. Frixione, V. Hirschi, F. Maltoni, et al. The automated computation of tree-level and next-to-leading order differential cross sections, and their

matching to parton shower simulations. *JHEP*, 1407:079, 2014.

[9] Serguei Chatrchyan et al. Observation of a new boson at a mass of 125 GeV with the CMS experiment at the LHC. *Phys. Lett.*, B716:30--61, 2012.

[10] J. H. Christenson, J. W. Cronin, V. L. Fitch, and R. Turlay. Evidence for the 2 pi Decay of the k(2)0 Meson. *Phys. Rev. Lett.*, 13:138--140, 1964.

[11] The ATLAS collaboration. Combination of ATLAS and CMS results on the mass of the top-quark using up to 4.9 fb^{-1} of $\sqrt{s} = 7$ TeV LHC data. 2013.

[12] Stefano Frixione, Paolo Nason, and Carlo Oleari. Matching NLO QCD computations with Parton Shower simulations: the POWHEG method. *JHEP*, 0711:070, 2007.

[13] Stefano Frixione, Paolo Nason, and Carlo Oleari. Matching NLO QCD computations with Parton Shower simulations: the POWHEG method. *JHEP*, 0711:070, 2007.

[14] Stefano Frixione, Paolo Nason, and Bryan R. Webber. Matching NLO QCD and parton showers in heavy flavor production. *JHEP*, 0308:007, 2003.

[15] Y. Fukuda et al. Evidence for oscillation of atmospheric neutrinos. *Phys. Rev. Lett.*, 81:1562--1567, 1998.

[16] D. Griffiths. *Introduction to Elementary Particles*. John Wiley & Sons, New York, USA, 1987.

[17] Peter W. Higgs. Broken Symmetries and the Masses of Gauge Bosons. *Phys. Rev. Lett.*, 13:508--509, 1964.

[18] S. Hoche et al. Matching parton showers and matrix elements. *hep-ph/0602031*, 2006.

[19] Takaaki Kajita. Atmospheric neutrino results from Super-Kamiokande and Kamiokande: Evidence for neutrino(mu) oscillations. *Nucl. Phys. Proc. Suppl.*, 77:123--132, 1999.

[20] Ian G. Moss. Higgs boson cosmology. 2015.

[21] Paolo Nason. A New method for combining NLO QCD with shower Monte Carlo algorithms. *JHEP*, 0411:040, 2004.

[22] K.A. Olive et al. Review of Particle Physics. *Chin.Phys.*, C38:090001, 2014.

[23] Torbjorn Sjostrand, Stephen Mrenna, and Peter Z. Skands. A Brief Introduction to PYTHIA 8.1. *Comput.Phys.Commun.*, 178:852--867, 2008.